AGU PUBLICATIONS

Global Biogeochemical Cycles

RESEARCH ARTICLE
10.1002/2015GB005180

Key Points:
- Largest record of δ30Si seasonal variations of settling diatoms in the Southern Ocean
- Seasonal surface DSi consumption and supply as well as particle settling rates are estimated
- Deep BSi fluxes are closely related to deep POC fluxes south to SAF

Supporting Information:
- Text S1, Figures S1–S8, Data Set S1 caption, and Table S1
- Data Set S1

Correspondence to:
I. Closset,
ivia.closset@locean-ipsl.upmc.fr

Citation:
Closset, I., D. Cardinal, S. G. Bray, F. Thil, I. Djouraev, A. S. Rigual-Hernández, and T. W. Trull (2015), Seasonal variations, origin, and fate of settling diatoms in the Southern Ocean tracked by silicon isotope records in deep sediment traps, *Global Biogeochem. Cycles*, *29*, 1495–1510, doi:10.1002/2015GB005180.

Received 2 MAY 2015
Accepted 8 AUG 2015
Accepted article online 13AUG 2015
Published online 25 SEP 2015

©2015. American Geophysical Union. All Rights Reserved.

Seasonal variations, origin, and fate of settling diatoms in the Southern Ocean tracked by silicon isotope records in deep sediment traps

Ivia Closset[1], Damien Cardinal[1], Stephen G. Bray[2], François Thil[4], Irina Djouraev[5], Andrés S. Rigual-Hernández[6], and Thomas W. Trull[2,3]

[1]Sorbonne Universités (UPMC, Pierre and Marie Curie University)-CNRS-IRD-MNHN, LOCEAN Laboratory, Paris, France, [2]Antarctic Climate and Ecosystems Cooperative Research Center, University of Tasmania, Hobart, Tasmania, Australia, [3]CSIRO Oceans and Atmosphere Flagship, Hobart, Tasmania, Australia, [4]Laboratoire des Sciences du Climat et de l'Environnement, CNRS, Gif-sur-Yvette, France, [5]IRD-Sorbonne Universités (UPMC, Pierre and Marie Curie University)-CNRS-MNHN, LOCEAN Laboratory, IRD France Nord, Bondy, France, [6]Department of Biological Sciences, Macquarie University, North Ryde, New South Wales, Australia

Abstract The Southern Ocean plays a pivotal role in the control of atmospheric CO_2 levels, via both physical and biological sequestration processes. The biological carbon transfer to the ocean interior is tightly coupled to the availability of other elements, especially iron as a trace-limiting nutrient and dissolved silicon as the mineral substrate that allows diatoms to dominate primary production. Importantly, variations in the silicon cycling are large but not well understood. Here we use δ^{30}Si measurements to track seasonal flows of silica to the deep sea, as captured by sediment trap time series, for the three major zones (Antarctic, AZ; Polar Frontal, PFZ; and Sub-Antarctic, SAZ) of the open Southern Ocean. Variations in the exported flux of biogenic silica (BSi) and its δ^{30}Si composition reveal a range of insights, including that (i) the sinking rate of BSi exceeds 200 m d^{-1} in summer in the AZ yet decreases to very low values in winter that allow particles to remain in the water column through to the following spring, (ii) occasional vertical mixing events affect the δ^{30}Si composition of exported BSi in both the SAZ and AZ, and (iii) the δ^{30}Si signature of diatoms is well conserved through the water column despite strong BSi and particulate organic carbon (POC) attenuation at depth and is closely linked to the Si consumption in surface waters. With the strong coupling observed between BSi and POC fluxes in PFZ and AZ, these data provide new constraints for application to biogeochemical models of seasonal controls on production and export.

1. Introduction

The Southern Ocean is a crucial component of the climate system where the oceanic biogeochemical cycles of carbon and silicon are closely connected through diatoms that dominate the primary production in the Antarctic Circumpolar Current (ACC) [*Ragueneau et al.*, 2000; *Assmy et al.*, 2013; *Tréguer and De La Rocha*, 2013]. As siliceous phytoplankton they have an absolute requirement for silicic acid (H_4SiO_4, hereafter referred to as dissolved silicon, DSi) to build their biogenic silica cell wall or frustule (amorphous $SiO_2 \cdot nH_2O$, hereafter referred to as biogenic silica, BSi). Diatoms are also the major exporters of organic matter and silica in the polar Southern Ocean where they dominate the modern BSi deposition [*Ragueneau et al.*, 2000]. Several processes occurring in the Southern Ocean impact on the biogeochemical properties of the low-latitude surface waters and on their biological productivity. Currently, the large DSi utilization by diatoms in the ACC, combined with the global overturning circulation, determines the functioning of the biological pump of low-latitude areas by maintaining a strong silicon limitation while still supplying other nutrients such as nitrate and phosphate to these regions [*Sarmiento et al.*, 2004]. Indeed, this complete consumption of DSi strongly contrasts with the low consumption of these other macronutrients, which appears to be driven by the strong seasonality of irradiance and mixing regimes of surface waters combined with the lack of micronutrients such as iron, so that the Southern Ocean represents the largest high-nutrient, low-chlorophyll (HNLC) area in the global ocean [*Martin*, 1990].

The physical and biogeochemical properties of surface waters in the ACC vary from north to south, and the Southern Ocean is divided into several oceanographic zones by different circumpolar fronts (Figure 1) [*Orsi et al.*, 1995]. The southern region is the Antarctic Zone (AZ) where biological production is not limited by

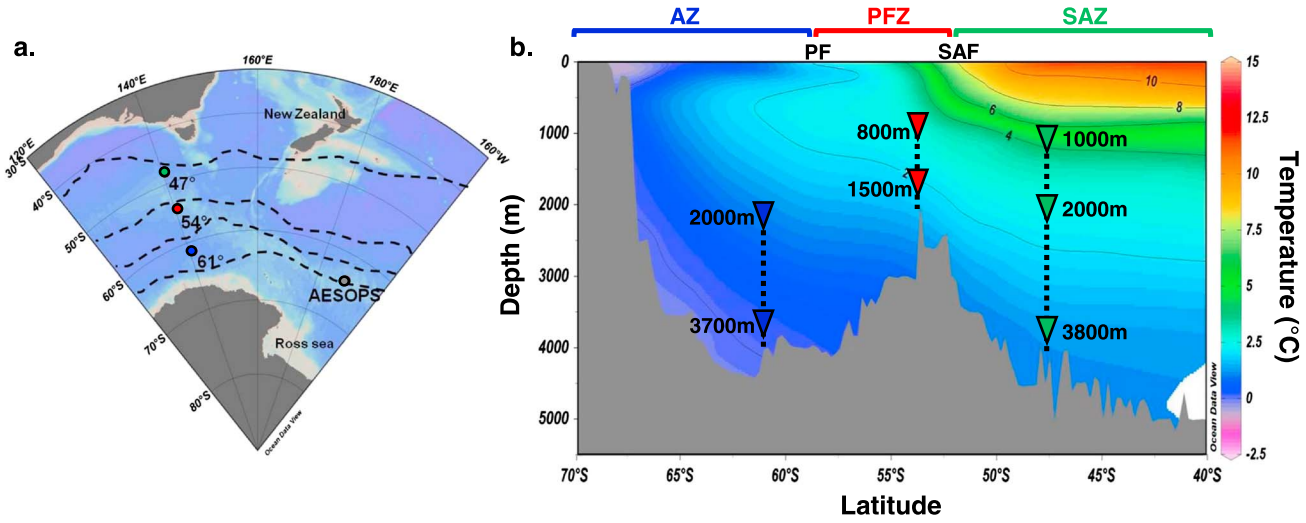

Figure 1. (a) Map showing the location of stations discussed in this study. From south to north, dotted lines represent the position of the Southern Antarctic circumpolar Current Front, Polar Front (PF), Sub-Antarctic Front (SAF), and Subtropical Front (STF), respectively. (b) Schematic view of the mooring configuration in relation to the bathymetry and the mean seawater temperature compiled from Electronic Atlas of World Ocean Circulation Experiment data.

macronutrient availability but mainly controlled by irradiance and iron concentrations [*Trull et al*., 2001a]. To its north, the Polar Front Zone (PFZ) lies between the Polar Front (PF) and the Sub-Antarctic Front (SAF). Here silicic acid concentrations remain high in the mixed layer (ML) until at least midsummer [*Trull et al*., 2001a; *Rintoul and Trull*, 2001]. Although the physical and biogeochemical properties of the AZ and PFZ differ in many ways, the dynamics of the primary production reveals some similarities such as strong seasonality and the predominance of diatoms [*Honjo et al*., 2000]. Farther north beyond the SAF, the Sub-Antarctic Zone (SAZ) is a region of transition from the cold nutrient-rich polar conditions to the warm nutrient-poor conditions of subtropical waters. In this zone, nitrate and phosphate concentrations remain moderately high, but DSi concentrations are low throughout the year and drop to nearly undetectable levels in summer [*Trull et al*., 2001a; *Rintoul and Trull*, 2001], limiting diatoms and favoring nonsiliceous autotrophic organisms such as coccolithophorids [*Kopczynska et al*., 2001; *De Salas et al*., 2011].

In order to study the marine silicon cycle, which is still marked by major uncertainties [*Tréguer and De La Rocha*, 2013], silicon isotopes are particularly useful because during silicification diatoms preferentially incorporate the lightest Si isotope (^{28}Si) into their cell wall [*De la Rocha et al*., 1997] leaving the stable isotope composition of DSi (expressed as δ^{30}Si; see section 2.4) relatively enriched in the heaviest Si isotope (^{30}Si). This leads to a progressive increase in δ^{30}Si of both substrate ($\delta^{30}Si_{DSi}$) and product ($\delta^{30}Si_{BSi}$) as the nutrient pool is consumed and results in the occurrence of a general inverse relationship between silicic acid concentration and δ^{30}Si in both DSi and diatom opal [e.g., *Varela et al*., 2004; *Cardinal et al*., 2005, 2007; *Fripiat et al*., 2011a]. Consequently, δ^{30}Si signatures can be used to trace the processes affecting both modern and past oceanic biogeochemical Si cycles [e.g., *De Souza et al*., 2014]. Several studies have used the δ^{30}Si signature preserved in diatom opal as a proxy for their Si utilization over geologic time in the Southern Ocean [e.g., *De la Rocha et al*., 1998; *Brzezinski et al*., 2002; *Beucher et al*., 2008; *Panizzo et al*., 2014], but only one study has investigated the variations of exported opal δ^{30}Si using 18 samples from sediment traps located in the Antarctic Zone of the Southern Ocean [*Varela et al*., 2004]. The mechanisms governing the seasonal variations of diatom δ^{30}Si signature and its transfer to depth have to be better constrained before δ^{30}Si of opal in the sediments can be used as a tracer for present and past changes in Si utilization.

In this paper, we investigate the spatial and seasonal variability of the silicon isotopic compositions of sinking particles collected in deep sediment traps at three sites in the Southern Ocean in the Antarctic, Polar Frontal, and Sub-Antarctic Zones. Our specific objectives are the following: (a) analyze the seasonality of $\delta^{30}Si_{BSi}$ flux in different zones of the ACC to infer information about the mechanisms and processes that govern surface Si dynamics and fate of diatoms in these regions and (2) identify the processes that control the transfer of $\delta^{30}Si_{BSi}$ to depth in order to fully validate its use in paleoceanographic records as a proxy for silicic acid utilization and diatom production in surface water.

2. Material and Methods

2.1. Sample Collection and Processing

Samples were collected from seven sediment traps (McLane Inc., Parflux 21-cup cylindrical funnels with baffles at the top and 0.5 m^2 collection surface area) deployed on three open ocean moorings along a north-south transect at 140°E in the Australian sector of the Southern Ocean. Stations were located in the AZ, PFZ, and SAZ at 61°S, 54°S, and 47°S, respectively. The shallowest traps were deployed at approximately 1 km below surface to minimize advection or swimmer problems (e.g., input of organisms that actively swim into the trap) and deepest traps approximately 700 m from the bottom of the seafloor to avoid the resuspension of bottom material. Both moorings in the SAZ and PFZ operated from 21 July 1999 to 29 August 2000, while in the AZ it ran from 26 November 2001 to 29 September 2002. For each mooring, cup rotation intervals were synchronized between traps and are given in the supporting information (Data Set S1). These intervals were set based on anticipated mass fluxes to allow a high sampling resolution during austral summer while lower time resolution was chosen during winter. Just before their deployment, sampling cups were filled with unfiltered seawater from the region mixed with a buffered solution of sodium tetraborate (1 g L^{-1}), sodium chloride (5 g L^{-1}), and mercury chloride (3 g L^{-1}). Tilt measurements show that the traps remain upright (typically within $< 3°$), and current speeds were generally below 12 cm s^{-1} [*Trull et al*., 2001b; S. G. Bray and T. W. Trull, annual report, unpublished data, 2000]. Thus, large hydrodynamic artifacts in the particles collections were not expected [*Buesseler et al*., 2007]. Following *Trull et al*. [2001b], who found little difference among similar traps using $^{230}Th_{xs}$, we did not estimate trap efficiencies because of the large uncertainties associated with this method [*Yu et al*., 2001]. Upon recovery, samples were sieved through 1 mm nylon mesh to remove swimmers and were split into 10 equal aliquots. One of these aliquots was filtered onto 0.45 μm pore size polycarbonate membrane filter, dried overnight at 60°C, ground in an agate mortar, and homogenized by repeated stirring. This aliquot was then subsampled for BSi concentration and Si isotopic measurements and stored in 6 mL glass vials for later analysis. Particulate organic carbon (POC) and mass fluxes were measured in separate aliquots, and a detailed description of this analytical procedure is given in *Trull et al*. [2001b] and discussed in *Rigual-Hernández et al*. [2015a].

2.2. Digestion and BSi Analyses

The collected trap material was solubilized using a two-step alkaline digestion adapted from *Ragueneau et al*. [2005]. Briefly, between 0.5 and 10 mg of particles was digested in Teflon tubes with 0.2 mol L^{-1} NaOH (pH 13.3) at 100°C for 40 min followed by neutralization with HCl (1 mol L^{-1}) to stop the reaction. A second and identical digestion was applied to estimate potential lithogenic contamination in the first leaching. Total particulate lithogenic Si is composed of biogenic and lithogenic components (mainly clay minerals), and the alkaline digestion can also solubilize a significant proportion of these aluminosilicates [*Ragueneau et al*., 2005] leading to a bias in biogenic Si fluxes and their Si isotopic signatures (see supporting information). Aluminum, a tracer of lithogenic source, was analyzed in the two leachates using an inductively coupled plasma mass spectrometer (ICP-MS; detection limit = 3.18 ppb) to quantify lithogenic Si contribution. Si concentrations were measured with a colorimetric method according to *Grasshoff et al*. [1999] and by ICP-MS on the same leachates as for Si isotopic composition. For each sediment trap sample, at least two full chemical replicates were processed. Average reproducibility of these replicates on BSi concentration was 9.0 ± 6.7% (1 sd, $n = 129$) which is well in agreement with the uncertainty estimated for this method (10%) [*Ragueneau et al*., 2005].

2.3. Purification

To avoid matrix effects during isotopic analyses, we purified the samples by cation exchange chromatography (BioRad cation exchange resin DOWEX 50W-X12, 200 to 400 mesh, in H^+ form) using a protocol described in *Georg et al*. [2006]. After purification, systematic analyses of major elements (such as Mg, Ca, Na, and Al) were performed by ICP-MS in order to ensure the sample purity prior to isotopic analyses. Si concentrations were also measured in the purified solutions to check for complete recovery. Moreover, five samples were analyzed by anionic chromatography to control the concentration of sulfate in the matrix, since it has been shown to induce a significant shift in isotopic measurements for SO_4^{2-}:Si weight ratios above 0.02 [*Van den Boorn et al*., 2009]. In these samples, sulfate concentration was systematically below the detection limit (<100 ppb) and leads to a SO_4^{2-}:Si ratio < 0.02 that does not require any correction for anionic matrix as proposed by *Hughes et al*. [2011] for rock digestion solutions.

Table 1. Mass Flux, Biogenic Silica and POC Flux, and Silicon Isotopic Composition of Particles (δ^{30}Si) Integrated Over the Sampling Period

Station	Depth (m)	Sampling Period	Mass Flux ($g\,m^{-2}\,yr^{-1}$)	BSi Flux ($mmol\,m^{-2}\,yr^{-1}$)	POC Flux ($mmol\,m^{-2}\,yr^{-1}$)	δ^{30}Si (‰)
AZ	2000	26 Nov 2001	95	1409	60.5	1.29
	3700	to 09 Oct 2002	79	1240	61.3	1.35
PFZ	800	21 Jul 1999	52	661	88.4	1.59
	1500	to 29 Aug 2000	33	477	50.9	1.49
SAZ	1000	21 Jul 1999	12	15	78.6	1.58
	2000	to 29 Aug 2000	18	25	139.0	1.65
	3800		15	14	94.3	1.52

2.4. Isotopic Measurements

Isotopic measurements were carried out on a Thermo Neptune^{+} multicollector inductively coupled plasma mass spectrometer (MC-ICP-MS; Laboratoire des Sciences du Climat et de l'Environnement, Gif-sur-Yvette) in dry plasma mode using Mg external doping to correct for the mass bias [*Cardinal et al*., 2003; *Abraham et al*., 2008]. Si solutions were introduced into the plasma via an Apex desolvating nebulization system equipped with a perfluoroalkoxy nebulizer (100 $\mu L\,min^{-1}$ uptake rate) without additional gas. Solutions were analyzed in medium-resolution mode ($M/\Delta M > 6000$) to find the optimum conditions to minimize the interference on the ^{30}Si peak. δ^{30}Si values obtained from the samples were calculated relative to the quartz standard NBS28 (RM8546). They were measured relative to an in-house standard quartz (Merck), which was not significantly different from NBS28 [*Abraham et al*., 2008], using a standard-sample-standard bracketing technique, and expressed as follows:

$$\delta^{30}\mathrm{Si}\,(‰) = \left[\frac{\left(^{30}\mathrm{Si}/^{28}\mathrm{Si}\right)\mathrm{sample}}{\left(^{30}\mathrm{Si}/^{28}\mathrm{Si}\right)\mathrm{standard}} - 1\right] \times 1000 \quad (1)$$

Interference-free measurement was ensured by checking that δ^{29}Si and δ^{30}Si for all the samples were consistent with the mass-dependent fractionation line (Figure S4). The signal was optimized to reduce the $^{14}N^{16}O$ interference on m/z 30 below 0.5% of the ^{30}Si peak. Measurements were performed on the left side of the peak where interference is minimal. Blanks were maintained below 1% of the main signal and were subtracted for each sample and standard. Typical analytical conditions are provided in Table S1. Long-term reproducibility and accuracy on δ^{30}Si values over the analytical procedure was calculated using the standard deviation of 109 analyses generated over 2.5 years of a secondary reference material (diatomite, $\delta^{30}\mathrm{Si} = 1.28 \pm 0.05$‰, $\delta^{29}\mathrm{Si} = 0.65 \pm 0.04$‰, 1 sd). This value is similar to the 1.26‰ δ^{30}Si signature of diatomite estimated during an interlaboratory comparison exercise by *Reynolds et al*. [2007]. Reproducibility of the full chemical procedure was estimated using at least one replicate of each sediment trap sample (chemical preparation plus isotopic measurements), and the average of reproducibility on duplicates δ^{30}Si was 0.05 ± 0.03‰ (1 sd, $n = 129$). Notably, this indicates that the BSi leaching procedure does not induce an additional bias and that uncertainty mostly originates from analytical measurements.

Since the alkaline digestion also dissolves LSi, and because it has a silicon isotopic signature significantly different from BSi (−2.3 to +0.1‰ compared to −0.3 to +2.6‰ for living diatoms) [*Opfergelt and Delmelle*, 2012], it is essential to estimate accurately the amount of LSi that contributes to the Si in each leachate used for isotopic measurement. In the cases where this fraction is significant, the δ^{30}Si value should be corrected from lithogenic contamination (see Text S1 and Figure S3). This was done only for SAZ samples since LSi contamination was negligible in the PFZ and AZ. Though significant, the corrections did not impact the shape of the seasonal profile or the overall interpretation of the SAZ data.

3. Results and Discussion

3.1. Latitudinal and Seasonal Variability of Exported Fluxes Along 140°W

The SAZ and PFZ moorings were programmed to sample over more than 1 year (405 days), while traps in the AZ collected particles for a shorter period (317 days). Considering the low particle fluxes registered at the onset and at the end of the mooring in the AZ, we can assume that fluxes in the nonsampled winter period were close to 0 [*Trull et al*., 2001b]. Consequently, the total deep mass flux varied by almost 1 order of

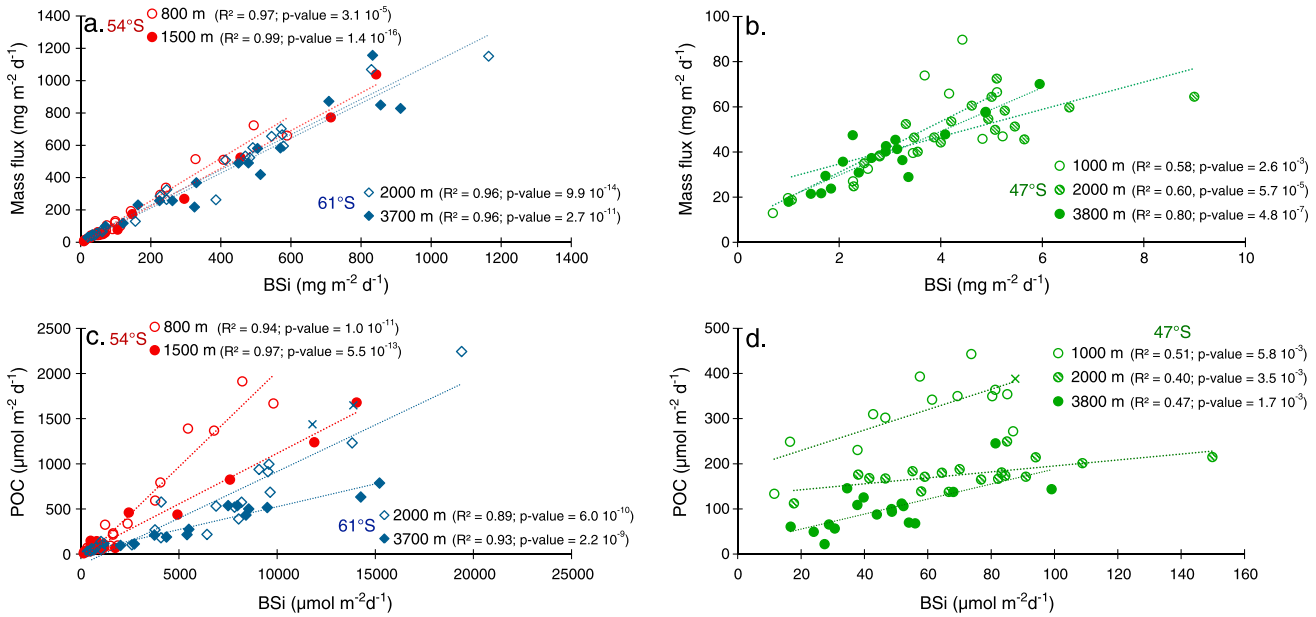

Figure 2. Correlations between the biogenic silica flux (BSi in mg SiO_2 m^{-2} d^{-1} or µmol m^{-2} d^{-1}) and mass flux (mg m^{-2} d^{-1}) or particulate organic carbon flux (POC in µmol m^{-2} d^{-1}) (a and c) in the Antarctic Zone (blue diamonds, blue crosses are outliers) and the Polar Front Zone (red dots) and (b and d) in the Sub-Antarctic Zone (green dots, green crosses are outliers). For mass versus BSi fluxes, slopes in Figure 2a are 0.066 ± 0.003 and 0.065 ± 0.005 for AZ 2000 m and 3700 m and 0.070 ± 0.002 and 0.079 ± 0.004 for PFZ 800 m and 1500 m, respectively; in Figure 2b 0.68 ± 0.17, 0.36 ± 0.07, and 0.58 ± 0.07 are for SAZ 1000 m, 2000 m, and 3800 m, respectively. For POC versus BSi fluxes, slopes in Figure 2c are 0.103 ± 0.009 and 0.050 ± 0.004 for AZ 2000 m and 3700 m and 0.211 ± 0.013 and 0.112 ± 0.005 for PFZ 800 m and 1500 m, respectively; in Figure 2d 2.26 ± 0.66, 0.85 ± 0.41, and 1.66 ± 0.44 are for SAZ 1000 m, 2000 m, and 3800 m, respectively.

magnitude from 12 g m^{-2} yr^{-1} in the SAZ (1000 m) to 95 g m^{-2} yr^{-1} in the AZ (2000 m), with PFZ values being intermediate (Table 1). The deep annual flux of biogenic silica exhibited even greater contrast, with the highest flux in the AZ (1408 mmol m^{-2} yr^{-1} at 2000 m) exceeding by 2 orders of magnitude the lowest flux in the SAZ (14 mmol m^{-2} yr^{-1} at 3800 m). Particulate organic carbon (POC) fluxes displayed an inverse pattern with the lowest flux in the AZ (61 mmol m^{-2} yr^{-1} at both depths) and the highest in the SAZ (139 mmol m^{-2} yr^{-1} at 2000 m). These fluxes are consistent with those measured by *Honjo et al.* [2000] in different stations from the same zones of the Southern Ocean in the Pacific sector (along 170°W). Overall, the total flux decreased with depth at all stations, except for the shallowest SAZ trap at 1000 m that displayed a lower flux than the two deeper traps. As particles produced in the ML do not necessarily sink vertically, shallower traps may undersample at current velocities that do not affect deeper traps [*Siegel et al.*, 1990]. Moreover, some evidence for horizontal advection of particles at mesopelagic depths has already been highlighted in this specific area [*Cardinal et al.*, 2001] probably originating from the Tasman Rise or Tasmanian shelf [*Rintoul and Trull*, 2001]. This statement could be confirmed by the occurrence of coastal and neritic diatoms in this trap [*Rigual-Hernández et al.*, 2015b]. Note that since the largest flux attenuation is often found shallower in the water column, these estimations reflected only the deep fluxes and differ considerably from particles exported out of the euphotic zone [*Boyd and Trull*, 2007; *Holzer et al.*, 2014].

Biogenic silica fluxes were highly correlated to mass fluxes ($R^2 > 0.9$, p value < 0.05, Figures 2a and 2b) and to POC fluxes ($R^2 > 0.85$, p value < 0.05, Figures 2c and 2d) in all the AZ and PFZ traps, as already reported in previous studies [e.g., *Honjo et al.*, 2000; *Trull et al.*, 2001b]. This results from the dominance of opal in the settling particles south of the SAF: the relative contribution of biogenic silica to the bulk flux ranged from 89% to 94% in the AZ and from 76% to 87% in the PFZ and could be mainly attributable to the occurrence of diverse assemblage of diatoms as counted in the same sediment traps [*Rigual-Hernández et al.*, 2015a]. South of the SAF, these organisms control the carbon transfer through depth. Figure 2 shows slope variations of the regressions between BSi and POC fluxes collected by the AZ and PFZ traps. These results indicate that the relationship between Si and C changed with depth. Indeed, the slope was significantly higher at 800 m (0.211 ± 0.013 in the PFZ) and decreased progressively with depth (from 0.112 ± 0.005 at 1500 m in the PFZ to 0.050 ± 0.004 at 3700 m in the AZ) as the relative contribution of POC to the flux decreased during the

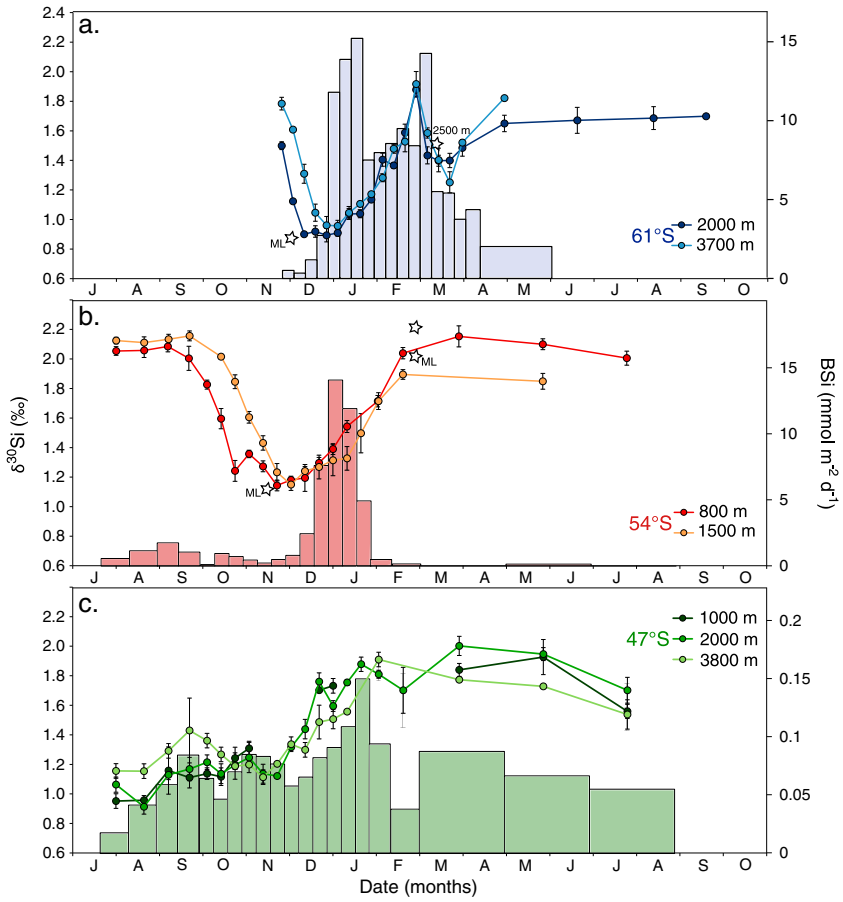

Figure 3. Seasonal variations of silicon isotopic composition (δ^{30}Si in ‰) of settling biogenic silica in comparison to the opal flux (BSi in mmol m^{-2} d^{-1}) in (a) the Antarctic Zone, (b) the Polar Front Zone, and (c) the Sub-Antarctic Zone. The BSi fluxes correspond to the sediment traps located at 2000 m in the AZ, 1500 m in the PFZ, and 2000 m in the SAZ. Stars correspond to δ^{30}Si measured in the mixed layer (ML) or at depth by *Cardinal et al.* [2007] in the same transect and *Fripiat et al.* [2012] in the Atlantic sector.

transport of particles through the water column. During this transfer, the organic matter continued to be remineralized in the mesopelagic and deep layers resulting in stronger attenuation of the POC fluxes compared to BSi. In the SAZ, biogenic silica fluxes corresponded only to 5.6 to 8.3% of the bulk fluxes. The correlations between BSi and mass flux were weaker, and slopes were significantly different (0.67 ± 0.02, 0.36 ± 0.07, and 0.58 ± 0.07 at 1000 , 2000 m, and 3800 m, respectively; Figure 2b.). This might partially reflect dissolution of diatom frustules in these warmer waters, which can be high in the ML [*Fripiat et al.*, 2011b; *Boyd et al.*, 2004]. Moreover, POC was poorly correlated to BSi (R^2 from 0.40 at 2000 m to 0.51 at 1000 m, Figure 2d) indicating that at these lower latitudes, siliceous organisms were not the main drivers of carbon transfer to depth. These observations highlight once again the crucial role of diatoms in the biological pump south of the SAF, while they should be less important in the SAZ, where nonsiliceous material dominated biogenic fluxes [*Ebersbach et al.*, 2011; *Trull et al.*, 2001b].

All the traps collected low total mass and BSi fluxes in early spring (Figure 3). As already observed by *Honjo et al.* [2000] in the Pacific sector, the onset of export was progressively delayed toward the south (from early September in the SAZ to mid-December in the AZ). Export fluxes showed different seasonal variations depending on the sampling zone. South of the SAF, fluxes reached a sharp maximum during austral summer. Particle fluxes in the AZ show two summer maxima separated by a period of reduced fluxes (Figure 3a). Here the fluxes collected by the deeper trap and shallower traps displayed similar seasonal patterns and magnitudes, indicating little dissolution of opal between 2000 and 3700 m. In the PFZ, the period of enhanced export occurred 15 days later at 1500 m compared to 800 m. In contrast, export during austral

winter exhibited a long period of very low particle flux from June to November and from March to October in the AZ and PFZ, respectively (Figures 3a and 3b). North of the SAF in the SAZ, particle and BSi fluxes were much lower and displayed a larger variability than those recorded in the two other zones (Figure 3c), as was also observed by *Trull et al*. [2001b] in 1997–1998 for the same SAZ and PFZ stations.

3.2. Biogeochemical Dynamics of Si in Regions Dominated by Diatoms South of the SAF

3.2.1. Seasonal Variations of Si Isotopic Composition of Sinking Diatoms

3.2.1.1. Spring

The seasonality of silicon isotopic composition of settling particles in the two stations south of the SAF is similar in many respects (Figures 3a and 3b). The lowest $\delta^{30}Si_{BSi}$ occurred at the onset of particle export. In the AZ, this light silicon isotopic composition (0.90 ± 0.01‰, $n = 2$, at 2000 m in December) is directly comparable to the $\delta^{30}Si$ of surface diatoms (0.85 ± 0.29‰) sampled above the sediment traps few weeks before [*Cardinal et al*., 2007]. For the PFZ, although not from the same year, the $\delta^{30}Si$ of surface diatoms above the PFZ mooring measured in mid-November 2001 (1.1 ± 0.02‰) [*Cardinal et al*., 2007] was also highly consistent with the sediment trap $\delta^{30}Si$ we measured for late November 1999 at 54°S (1.14 ± 0.04‰). These light $\delta^{30}Si$ can thus be considered as spring values for diatoms blooming south of the SAF. Since, for each mooring, this signature is not significantly different among the depths or from surface waters, we can furthermore assume that dissolution processes occurring during settling did not affect the $\delta^{30}Si$ of BSi. The constancy of Si isotopic signature of BSi with depth has been already observed for suspended particles of the Atlantic sector [*Fripiat et al*., 2012] as well as for the U.S. JGOF Antarctic Environment and Southern Ocean Process Study (AESOPS) sediment traps in the Southern Ocean south of New Zealand [*Varela et al*., 2004].

3.2.1.2. Summer

After these initial low values, the $\delta^{30}Si$ signatures became gradually heavier as the flux of BSi collected in the cups evidenced enhanced production and export of particles from the surface waters (Figures 3a and 3b). This reflects the response to the BSi production and export of diatoms through the ML, because $\delta^{30}Si$ signatures of both the remaining seawater and newly formed diatoms will increase concomitantly with the progressive increase of nutrient consumption and Si limitation in surface waters. Diatoms preferentially incorporate the lightest Si isotope (^{28}Si) into their cell wall [*De la Rocha et al*., 1997] leaving the $\delta^{30}Si_{DSi}$ enriched in the heaviest Si isotope (^{30}Si). This leads to a progressive increase in $\delta^{30}Si$ of both substrate ($\delta^{30}Si_{DSi}$) and product ($\delta^{30}Si_{BSi}$) as the nutrient pool is consumed and results in the occurrence of an inverse relationship between silicic acid concentration and $\delta^{30}Si$ of both silicic acid and diatom opal [e.g., *Cardinal et al*., 2005, 2007; *Varela et al*., 2004; *Fripiat et al*., 2011c]. This relation is generally described using two different fractionation models (Rayleigh versus steady state) [*Fry*, 2006]. However, both models are very sensitive to the initial conditions (winter DSi concentration and $\delta^{30}Si_{DSi}$) [*Cardinal et al*., 2005]. Since we did not have direct information about these initial conditions, it was too speculative to compare in a simple way our data with these theoretical models. Moreover, neither of these models was able to describe correctly the seasonal variations of $\delta^{30}Si_{BSi}$ (data not shown). In addition to the uncertainty on initial conditions, this might be due to (i) the lack of constraint on the evolution of the relative utilization of the ML DSi with time and/or (ii) the system that cannot be considered as behaving according to one "Rayleigh" or one "steady state" system all year long. The time evolution of $\delta^{30}Si$ in sediment traps needs to be investigated using a modeling approach different from Rayleigh or steady state, cf., for instance, the one proposed by *Fripiat et al*. [2012]. This work is still ongoing and will be discussed in a specific paper.

Focusing on the overall magnitude of the seasonal changes, we note the following comparisons to previous work. The seasonal development of the diatom bloom in the Pacific sector of the Southern Ocean was followed in 1998 by *Nelson et al*. [2001] and showed a silicic acid depletion of more than 40 μmol L^{-1} in the AZ surface waters. In the PFZ, the high $\delta^{30}Si$ signature (2.04 ± 0.04‰ in February) was in the same range as those measured in the Atlantic sector in the end of summer (2.00 ± 0.02‰ in the ML and 2.29 ± 0.06‰ at 1068 m) [*Fripiat et al*., 2012] suggesting that the spatial scale of the summertime DSi depletion and potential Si limitation in the PFZ may be nearly circumpolar. Here both the lower silicic acid concentrations and the occurrence of some degree of Si limitation north of the PF explain the heavier $\delta^{30}Si$ signals at 54°S compared to the AZ at 61°S (Figure 3b).

3.2.1.3. Autumn

In March, the settling particles became suddenly lighter by −0.8 to −1.0‰ in the AZ (Figure 3a). Such a huge shift was also observed in sediment traps in the AZ along 170°W [*Varela et al*., 2004] and suggests the

occurrence of vertical mixing events supplying waters with high silicic acid content and light $\delta^{30}Si$ into the euphotic zone. Indeed, during the AESOPS program *Brzezinski et al.* [2001] and *Nelson et al.* [2001] measured relatively elevated DSi concentrations during February and March between 60.5°S and 65°S. They proposed that these mixing events ultimately led to the collapse of the bloom in the AZ [*Brzezinski et al.*, 2001]. The $\delta^{30}Si_{BSi}$ collected in our shallower trap during this period (1.43 ± 0.05‰) was also highly consistent with the $\delta^{30}Si$ of suspended particles measured at 2500 m in the Atlantic sector by *Fripiat et al.* [2012] (1.42 ± 0.2‰ in March 2008), suggesting that the influence of mixing events may be widespread in the AZ and recurrent over years. By contrast, no $\delta^{30}Si$ decline was observed at the end of summer in the PFZ suggesting that the demise of the bloom here may not be associated with mixing events or variations in the Mixed Layer Depth (MLD) as in the AZ but might more probably be controlled by iron and/or silicic acid limitation in the surface water [*Boyd et al.*, 1999].

3.2.1.4. Winter

The silicon isotopic composition of settling particles remained strikingly heavy and constant between May and October (1.7 ± 0.02‰ averaged) in the AZ and between February and October (2.1 ± 0.05‰ averaged) in the PFZ, at a time when winter deep convection takes place (Figures 3a and 3b) [*Sallée et al.*, 2006]. The $\delta^{30}Si$ values only started to decrease at the beginning of spring when the BSi flux increases as a result of the initiation of export production from surface water. Indeed, the same heavy signature was observed in the single cup that collected particles during winter in the AZ along 170°W [*Varela et al.*, 2004]. The authors proposed at that time that the material has arrived in this cup early during the sampling time interval and corresponded likely to frustules sinking before the occurrence of winter night. Since we recorded this heavy $\delta^{30}Si$ in several cups throughout the winter period (4 cups at 2000 m from mid-April to October 2002), this cannot be the case in our samples. So these heavy $\delta^{30}Si$ signatures are representative of the low flux of diatoms reaching the traps during the nonproductive period. In a recent study, *Sutton et al.* [2013] pointed out that Si isotope fractionation by polar and subpolar diatoms is species dependent. The heavy $\delta^{30}Si$ observed in winter might be attributed to a succession of different diatom assemblages. However, in our case the species *Fragilariopsis kerguelensis* always dominated the flux of particles in all the traps located south of the SAF [*Rigual-Hernández et al.*, 2015a]. Moreover, *Grasse et al.* [2013] reported in the eastern equatorial Pacific the lowest fractionated surface waters in the upwelling area which was dominated by *Chaetoceros* spp., expected to induce the highest fractionation according to *Sutton et al.* [2013]. Our data presented here also suggest that other factors than species are the dominant control on the Si isotope composition of the exported particles. Diatoms bearing an isotopic signature typical of late summer and that continue to settle in deep traps several months after the end of the growing season might explain such heavy $\delta^{30}Si$. These diatoms might be empty, broken, and/or partly dissolved due to the influence of trophic interactions that could be important during the postbloom period and that could help to retain particles in the ML. Indeed, both mesozooplankton and microzooplankton communities (such as copepods and heteroflagellates, respectively) are likely to control significantly the fate of diatoms. In his conceptual scheme of the bloom dynamics in the Southern Ocean, *Quéguiner* [2013] suggests that zooplankton can in turn transform their fecal pellets into smaller particles that are easily retained in the ML where bacteria could progressively degrade the organic matter associated to this material. Then, while no study was conducted on the particle size spectra in our samples, we can reasonably assume that winter fluxes were composed of small particles and diatom fragments that have a heavier $\delta^{30}Si$ signature compared to "fresh" diatoms (on average 0.5‰ higher than normal range for diatoms) [*Egan et al.*, 2012]. Alternatively, such weak and late diatom flux could originate from diatoms exported out of the ML at the end of the growth season, e.g., along with medium to small aggregates and that would have been released in mesopelagic waters as smaller fragments during the remineralization of these aggregates. This happens to be the case, for instance, with microbarites (1–5 μm) precipitated in organic aggregates and then released as "suspended particles" in mesopelagic waters. A fraction of these microparticles remain even during winter and constitute the background particulate Ba signal [*Cardinal et al.*, 2005]. Diatom fragments, likely to be larger than microbarites, would have then settled very slowly and could illustrate a continuum between the conventional two categories of settling and suspended particles.

All these processes which are not exclusive would contribute to generate a weak flux of isotopically heavy diatoms as observed in the trap. By summing all the BSi fluxes collected in the traps during winter, we can estimate this BSi stock to be 0.24 mol m^{-2} and 0.28 mol m^{-2} in the AZ and PFZ, respectively. These values in both zones are consistent with the BSi stock measured in the euphotic zone at the end of summer along

the AESOPS transect (170°W in the Pacific sector): from 0.17 to 0.22 mol m^{-2} in the AZ in March 1998 [*Brzezinski et al*., 2001; *Sigmon et al*., 2002]. BSi standing stock in the PFZ (from 0.05 to 0.08 mol m^{-2}) was, however, lower than those required to maintain the flux of siliceous material we measured during the whole winter at 54°S. Since AESOPS values were integrated over the euphotic layer (from 100% to 1% of the surface photosynthetically active radiation = PAR), they did not take into account the occurrence of biogenic material (usually dominated by diatoms) just below the ML as already observed in summer and autumn at our PFZ mooring station [*Parslow et al*., 2001]. In March, this subsurface opal accumulation could be located at depths greater than 100 m. In the Indian sector HNLC waters, *Mosseri et al*. [2008] measured during the bloom offset BSi concentrations (from 0.2 to 0.5 mol m^{-2} integrated over 200 m) that were comparable to our estimations (note that this range of values is also similar in the iron-fertilized stations located over the Kerguelen Plateau —0.2 to 0.8 mol m^{-2}). Thus, we can reasonably assume that the BSi stock estimated from the sum of opal fluxes collected in winter cups can be explained by the BSi stock that can be found in the ML after the demise of the summer bloom in both the AZ and PFZ.

3.1.2.5. Winter-Spring Transition

Early spring, the $\delta^{30}Si$ signal started to decrease progressively from 1.50 ± 0.04‰ to 0.89 ± 0.04‰ in the AZ and from 2.1 ± 0.04‰ to 1.14 ± 0.04‰ in the PFZ. The progressive lightening of silicon isotopic composition of settling particles implies that a mix between old and isotopically heavy diatom fragments and recent particles with light $\delta^{30}Si$ signature formed during the spring bloom with an increasing contribution of fresh particles to this mix. Considering that the heaviest ("H") winter $\delta^{30}Si$ value is representative of the detritic Si isotopic signal ($\delta^{30}Si_{(H)}$ = 1.78 ± 0.05‰ and 1.50 ± 0.04‰ at 3700 m and 2000 m respectively in the AZ and $\delta^{30}Si_{(H)}$ = 2.16 ± 0.03‰ and 2.08 ± 0.04‰ at 1500 m and 800 m respectively in the PFZ) and that the lowest ("L") spring $\delta^{30}Si$ value corresponds to the signature of "fresh diatoms" ($\delta^{30}Si_{(L)}$ = 0.96 ± 0.06‰ and 0.89 ± 0.04‰ at 3700 m and 2000 m respectively in the AZ and $\delta^{30}Si_{(L)}$ = 1.15 ± 0.04‰ and 1.14 ± 0.04‰ at 1500 m and 800 m respectively in the PFZ), we are able to estimate the contribution of new-formed particles in each of the early spring cups as follows:

$$X_{(new)} = \frac{\delta^{30}Si_{Cup} - \delta^{30}Si_{(H)}}{\delta^{30}Si_{(L)} - \delta^{30}Si_{(H)}} \times 100 \quad (2)$$

where $X_{(new)}$ is the proportion of fresh biogenic silica in percent and $\delta^{30}Si_{Cup}$ is the silicon isotopic composition of the particles in the cup.

Using this equation in the cups that collected material early spring, we have estimated an increasing proportion of these new diatoms from 21% to 90% in the AZ and from 14% to 92% in the PFZ (example for the 2000 m and 1500 m traps in the AZ and PFZ, respectively) (Data Set S1). This observation is consistent with the increasing production in surface water (Figures S5 and S6) and with the following discussion about the processes that control the settling of diatoms in the water column (see section 3.2.2). The combination of elevated light levels and shallower MLDs allows the development of a diatom-dominated bloom with maximum biomass and productivity centered between the southern edge of the PF and 66°S [*Nelson et al*., 2001; *Grigorov et al*., 2014]. Note that the $\delta^{30}Si$ values decreased 2 months earlier at 54°S than at 61°S and in the same way started to increase 1 month earlier in spring (Figure 3b). These two observations reflect the seasonal progression of bloom development and then Si consumption that starts first in the subantarctic waters located north of the PFZ and spreads southward during summer as already revealed by *Brzezinski et al*. [2001] and *Nelson et al*. [2001] in the Pacific sector of the Southern Ocean.

3.2.2. Settling Rates

The progressive consumption of H_4SiO_4 which should control to first order the observed silicon isotopic seasonal variations is likely associated with a succession of different phytoplankton (and zooplankton) populations in the ML [*Quéguiner*, 2013] that produce finally a succession of different type of particles sinking with distinct velocities. Settling rate is a key parameter regarding the fate of organic matter produced in the ML which is highly variable and difficult to assess [*Boyd and Trull*, 2007]. Since biological and physical degradation processes (e.g., bacterial respiration and grazing) will affect more efficiently slow-sinking particles [*Goutx et al*., 2007], the rate at which a particle will sink through the water column will strongly affect its transfer efficiency to depth and thus the efficiency of the biological carbon pump [*Trull et al*., 2008; *Iversen and Ploug*, 2013].

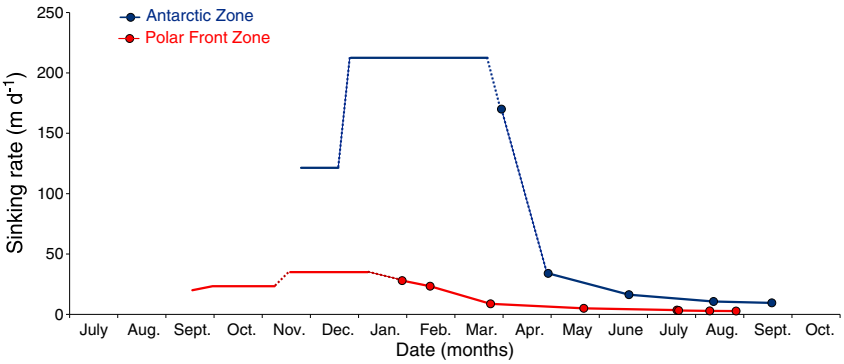

Figure 4. Seasonal variations of sinking velocities of particles estimated from δ^{30}Si signatures of settling diatoms in the Antarctic Zone (in blue) and in the Polar Front Zone (in red).

The settling velocity of particles is commonly expressed using Stokes law where it mainly depends on size and excess density of particles (partly controlled by porosity and particle composition). However, recent studies have revealed that no simple physical formulation seems to be able to explain the wide range of sinking rates observed in the ocean (from less than 1 m d^{-1} to more than several hundred m d^{-1} [*Turner et al.*, 2002; *Trull et al.*, 2008; *Stemmann et al.*, 2004; *MacDonnell and Buesseler*, 2010; *Laurenceau-Cornec et al.*, 2015a, 2015b]). Direct measurements of this crucial parameter have been performed in situ using specific sediment traps [e.g., *Trull et al.*, 2008] or optical cameras [e.g., *Asper and Smith*, 2003], but they remain very scarce for the open ocean. In this study we propose to estimate the diatom settling rates using time series analysis of δ^{30}Si of particles in sediment traps located at different depths.

Since the isotopic composition of BSi transferred to depth was comparable to the one leaving the ML (Figure 3a) and integrated δ^{30}Si do not vary with depth (Table 1), we can assume that the δ^{30}Si signature of settling particles was not affected by any significant dissolution processes during transfer through the water column. Then, each pool of diatoms produced at one time in the ML should have the same δ^{30}Si in both the shallowest and deepest trap. By comparing the time lag between the occurrences of particles with the same δ^{30}Si at different trap depths, we can calculate the sinking velocity of this pool of diatoms between the two targeted depths. Note that the values estimated using this approach represent only deep settling speeds since they were not estimated from the ML but in the water layer between two deep sediment traps. Moreover, it is important to keep in mind that because of the duration of the sampling for each cup (at least 8 days), the rates calculated in this study correspond to a lower limit estimate of sinking velocities.

In the AZ, the δ^{30}Si values were similar in the shallowest and deepest traps from January to April suggesting that particles sank quickly through the water column, coinciding with the maximum of BSi flux. Such rapid sedimentation during the summer bloom period (W_{bloom}) may be expressed by dividing the distance between the traps by the cup sampling time interval, i.e., at least 213 m d^{-1} between 2000 and 3700 m (Figure 4). In the PFZ, we observed a small time lag between the isotopic signatures of material collected in both traps from December to mid-February. Indeed, the δ^{30}Si started to decrease between cups 3 and 4 in the shallowest trap while it did not show any significant drop before cup 4 at 1500 m. Similarly, it reached its minimum value one cup later in the deepest trap in spring (Figure 3b). This time lag in particle fluxes could also be observed in Figure S6 where BSi fluxes reach their maximum one cup earlier at 800 m. Taking into account this 10 day offset in the sampling time interval, sinking rates of particles may be estimated using the same approach as in the AZ and were at least 35 m d^{-1} between 800 and 1500 m (Figure 4). Both values (213 m d^{-1} and 35 m d^{-1} at 61°S and 54°S, respectively) were in the range of published values for marine snow composed of diatom flocs (10 to several hundreds m d^{-1} [*Turner*, 2002; *Trull et al.*, 2008; *Laurenceau-Cornec et al.*, 2015b]). While the sinking velocity of single diatom cells or chains is in the range of 1 to 10 m d^{-1} [*Turner*, 2002], this speed could be increased by several orders of magnitude in the case of diatom aggregates. Indeed, during austral summers (1999, 2001, and 2007), the flux of particles and diatom composition in the ML at these two latitudes were mainly composed by the highly silicified diatom *Fragilariopsis kerguelensis* [*De Salas et al.*, 2011; *Rigual-Hernández et al.*, 2015a] that are known to form chains and may reach rapidly the traps as fast-sinking phytodetrital and/or fecal aggregates as already proposed by

Ebersbach et al. [2011], *Grigorov et al*. [2014], and *Laurenceau-Cornec et al*. [2015a] for the PFZ site, the AESOPS transect, and the Kerguelen Plateau, respectively.

Since we have shown that winter BSi fluxes originate from late summer, in order to sustain such fluxes over the whole winter, the sinking velocities of particles should be low. We have calculated these rates (W_{winter}) by dividing the distance between the traps with the sum of the cup opening durations during the nonproductive period. This imposes an exponential decrease of the rates with time which might not reflect reality, but this approach is supported by the winter δ^{30}Si signatures. Winter settling rates estimate decrease from 34 to 9.5 m d^{-1} at 61°S and from 23 to $<$ 3 m d^{-1} at 54°S (Figure 4). These estimates correspond to sinking rates of single phytoplankton cells (from $<$ 1 to tens of m d^{-1} [*Turner*, 2002]) and strongly differ from the high velocities of marine snow. As already discussed previously, this low winter flux might be mainly composed of broken or partly dissolved diatoms that should sink as single cell or small aggregates.

The progressive lightening of δ^{30}Si signature in early spring is delayed between the shallowest and deepest trap (approximately 6 and 20 days at 61°S and 54°S, respectively, Figures 3a and 3b) implying that particles have slower velocities than those of summer aggregates. Indeed, taking into account this delay and using the same relation as used to calculate W_{bloom}, we estimate sinking rates of spring particles (W_{spring}) of at least 121 and 23 m d^{-1} in the AZ and PFZ, respectively. Even if these values were lower than those estimated for the summer bloom, they were still in the range of published values for sinking aggregates. Thus, it is possible that diatoms growing during the early spring bloom form smaller and more "fluffy" phytodetrital aggregates than the dense and compact aggregates produced during the intense summer bloom. Indeed, particles produced during the growing stage of the bloom may be composed of relatively unprocessed and fresh material, while later in the season, aggregates might become more compact and could contain more zooplankton mediated particles [*Thornton*, 2002]. During their sedimentation through the water column, these spring fluffy aggregates may scavenge small and isotopically heavy particles that were retained in surface and intermediate waters during austral winter. Efficient adsorption of suspended particles by settling aggregates has already been observed in the ML [*Passow et al*., 2001; *Iversen and Ploug*, 2010]. This support the idea of a mixing between old and slow-sinking particles and fresh and fast-sinking aggregates in the cups and also the progressive lightening of silicon isotopic composition of sinking particles associated to an increasing contribution of fresh and isotopically light diatoms.

Note that in the PFZ W_{spring}, W_{bloom} and W_{winter} were systematically lower than those estimated for the AZ (Figure 4). Since phytoplankton populations were dominated by the same diatom species (*Fragilariopsis kerguelensis*) [*Rigual-Hernández et al*., 2015a, 2015b] at both latitudes, differences in planktonic community structure cannot explain these observations. However, samples collected in 1999–2000 in the PFZ were very rich in small and lightly silicified fragments compared to those sampled in the AZ or during different years [*Rigual-Hernández et al*., 2015a]. Most of these fragments correspond to remains of frustules of *Pseudo-nitzschia* species, setae of *Chaetoceros* spp., and other thin-shelled species and could suggest that some type of intense "grazing event" might have occurred in the surface water that year. Note that these contrasted sinking velocities might also be due to a sampling artifact since the traps were located at a much lower depth in the PFZ (800 and 1500 m) than in the AZ (2000 and 3700 m). Indeed, as the particles sink through the water column, the organic matter is remineralized by microbial activity. This process might increase the relative content of minerals and the density excess of aggregates (ballast effect) that will accelerate their sedimentation with depth [*Armstrong et al*., 2002; *Iversen and Ploug*, 2010]. However, given that all the particles already have very low POC contents, this may not be the dominant effect, and an alternate possible explanation is that the Antarctic Zone particles are denser owing to greater compaction during their physical and biological initial aggregation in the surface mixed layer.

The overall seasonal picture that emerges from our estimations of particle sinking rates is that both sites show higher sinking rates at times of higher fluxes (Figure 4). To the extent that higher sinking rates allow particles to experience less degradation during their transit to the traps, this implies the possibility of more efficient POC transfer during high flux periods. This does appear to be the case for the Antarctic Zone, where POC/BSi ratios were found to be somewhat elevated during the summer high flux period, although POC contents were nonetheless very low ($<$1.5% of dry mass) and thus POC export also small [*Rigual-Hernández et al*., 2015a].

3.3. Biogeochemical Dynamics of Si in the SAZ

3.3.1. Variations of Si Isotopic Composition of Sinking Diatoms

North of the SAF, the silicon isotopic composition of settling particles was 0.9 ± 0.03‰ at the end of winter and reached a maximum of 1.8 ± 0.03‰ in March when the BSi export at 2000 m began to decrease (Figure 3c). The range of δ^{30}Si values was comparable to those measured in the AZ even though these two zones exhibit different DSi concentrations and phytoplankton composition assemblages in their own surface waters. This latitudinal trend was already observed in the Atlantic sector of the Southern Ocean [*Fripiat et al*., 2012] and could result from a concomitant decline of silicon isotopic composition of surface seawater δ^{30}Si as observed for the same transection in late spring 2001 [*Cardinal et al*., 2005].

Since BSi fluxes were much lower and variable in the SAZ, the δ^{30}Si signature of sinking particles displayed a larger variability than in the AZ and PFZ (Figure 3). This variability could be associated to a greater instability of the ML. The surface layer in the SAZ is weakly stratified [e.g., *Sallée et al*., 2006], which translates into both very deep ML (Figure S8) and large intraseasonal variability. Variability in the ML can arise from multiple sources including mesoscale activity [*Rintoul and Trull*, 2001], anomalous air-sea buoyancy fluxes [*Schulz et al*., 2012], or anomalous burst of wind-induced cross-frontal Ekman transport [*Sallée et al*., 2006]. In addition to deepening the ML, cross-frontal transport impacts the nitrogen isotopic composition of nitrate in different parts of the SAZ [*Sigman et al*., 1999]. Altogether, the weak stratification and the burst of northward cross-frontal transport result in temporary nonoptimal light conditions for phytoplankton growth, as well as pulses of new and isotopically light silicic acid in surface waters.

Even if the seasonal cycle of δ^{30}Si at 47°S was more scattered than in the two other zones, we clearly see that the δ^{30}Si of BSi increased as the bloom developed in surface water (Figure 3c). Relating this trend to the strong seasonality of the MLD that occurs in the SAZ is tempting. Indeed, several studies have evidenced that the MLD in the SAZ exhibits large seasonal variability with deep mixed layers before November (>400 m) and stable and shallow mixed layers (<50 m) from December to March (Figure S8 [*Rintoul and Trull*, 2001; *Dong et al*., 2008; *Weeding and Trull*, 2014]). Thus, the combination of deep MLD (200 to more than 500 m) and cross-frontal transport of surface waters in winter and early spring will prevent the development of diatoms, maintaining their relatively lighter silicon isotopic composition. On average, the δ^{30}Si values of settling particles increased slightly from 0.89 ± 0.05‰ in August to 1.10 ± 0.00‰ in November (Figure 3c). It was only in summer when the ML is much shallower (≈35–45 m) and the stratification more stable and when phytoplankton experiences conditions suitable to grow that silicon isotopic composition of particles became significantly heavier (from 1.10 ± 0.00‰ in November to 1.80 ± 0.11‰, Figure 3c).

However, this trend could also be associated to the increasing relative abundance of diatom frustules in the siliceous phytoplankton assemblages compared to other siliceous organisms such as silicoflagellates and/or radiolarians (from less than 60% in August to more than 90% in December, A. S. Rigual-Hernandez, unpublished data). Radiolarians are siliceous planktonic organisms that can have lower δ^{30}Si compared to diatoms, but due to the scarcity of measurements, the range of radiolarian δ^{30}Si is unknown. To our knowledge, only three studies have indirectly addressed this issue. *Ding et al*. [1996] have measured light silicon isotopic composition (−0.2 to 0.3‰) in sediments dominated by radiolarians. Using ultrasonic microseparation of particles, *Egan et al*. [2012] have also observed systematically lighter δ^{30}Si value (sometimes even negative) in the size fraction > 50 μm where radiolarian occurs. In contrast, *Hendry et al*. [2014] recently measured a wide range of δ^{30}Si for radiolarian (from 0.73 to 2‰) in the Sargasso Sea sediments. Hence, the trend of silicon isotopic composition of BSi in early spring could reflect the concomitant effect of a shift in water ventilation as well as a change in the composition of settling particles.

3.4. Implication for Interpretation of Sedimentary Records

From a palaeoceanographic perspective, diatom δ^{30}Si preserved in sediment core material can be used as a proxy of diatom silicic acid utilization, with high δ^{30}Si reflecting high nutrient consumption [*De La Rocha et al*., 1998; *De La Rocha*, 2006; *Varela et al*., 2004; *Beucher et al*., 2008; *Egan et al*., 2012; *Elhert et al*., 2012; *Etourneau et al*., 2012]. These studies linked the δ^{30}Si of opal with the isotopic signature of surface seawater and the extent of DSi depletion in the ML by using either closed-system or open-system models. It is currently not obvious which model best describes the silicon mass and isotopic variations in the modern Southern Ocean and is the most appropriate to reconstruct past processes from exported particle signatures.

In the SAZ, the isotopic signature of exported opal integrated over the whole season ($\int\delta^{30}Si = 1.65‰$, Table 1) corresponds to a complete Si depletion in the ML and is consistent with the fact that $\delta^{30}Si$ of exported BSi records the extent of DSi consumption in the ML (i.e., it reflects the period when diatoms are growing driving H_4SiO_4 concentration in surface waters to its minimum annual value [*Egan et al*., 2012]). Moreover, this integrated isotopic signature of exported opal falls within the range of previous modern sedimentary records (e.g., from 1.65 to 2‰ during the Holocene [*Beucher et al*., 2008] and from 1.36 to 2.07‰ in core top material [*Egan et al*., 2012]).

The isotopic signatures of exported opal integrated over the whole season ($\int\delta^{30}Si$) are 1.59‰ and 1.29‰, in the PFZ and AZ, respectively, consistent with the range of published core top records (from 1.21 to 1.68‰ in PFZ and from 1.14 to 1.58‰ in AZ [*Egan et al*., 2012]). These integrated $\delta^{30}Si$ signatures can be associated to a strong depletion of the initial DSi pool consistent with the values observed at the end of the productive period in the PFZ (from 1.8 to 4.0 $\mu mol\,L^{-1}$ [*Trull et al*., 2001a; *Fripiat et al*., 2011a]) and AZ ($\approx$10 $\mu mol\,L^{-1}$ [*Trull et al*., 2001a; *Brzezinski et al*., 2001]). The $\int\delta^{30}Si$ of exported particles that is preserved in the sediments likely reflects the Si consumption by diatoms and can be used to reconstruct past H_4SiO_4 concentrations prevailing at the end of the productive period.

4. Conclusions

Our study addressed the seasonal evolution of the silicon isotopic signature of sinking biogenic silica in different zones of the Southern Ocean. As already observed during previous studies [*Varela et al*., 2004; *Fripiat et al*., 2012], the $\delta^{30}Si$ signature of diatoms in our samples was well preserved through the water column and was closely linked to the Si consumption in surface waters, validating the use of this proxy to reconstruct past Si utilization by diatoms in the ML. South of the SAF, the isotopic composition of particles was not altered despite the strong BSi and POC flux attenuation observed in the mesopelagic and deep layers. During this transfer, organic matter was still remineralized leading to a stronger attenuation of the POC fluxes compared to BSi below 2000 m.

This study suggests that diatoms are closely related to the carbon transfer to the deep Southern Ocean since opal dominated the particle flux (more than 75% of the flux) and was strongly correlated to the POC flux south of the SAF. In the SAZ, siliceous organisms were not the main drivers of carbon export since BSi contributed less than 10% of the biogenic fluxes. These observations support the idea that diatoms played a key role in the control of the biological pump south of the SAF.

We confirm and complete the seasonal trend observed in the single previous work that investigated the $\delta^{30}Si_{BSi}$ from the sediment trap samples in the AZ [*Varela et al*., 2004]. Combining these results with two other data sets in the PFZ and the SAZ, we have highlighted that the SAZ has a distinct silicon isotope and mass balance than regions located south of the SAF. In this latter region, the Si supply:Si uptake ratio was extremely low in summer and the $\delta^{30}Si_{BSi}$ increased exponentially during this period, as the silicic acid was consumed in surface waters. These observations were highly consistent with the simulation proposed in the AZ and PFZ by *Fripiat et al*. [2012]. Because of its high mesoscale activity and its low DSi concentrations in surface waters, the SAZ exhibit a higher BSi dissolution-production ratio and a higher Si supply:Si uptake ratio that may reduce the apparent fractionation factor. The $\delta^{30}Si_{BSi}$ was thus more variable but shows a clear increasing linear trend during the year.

We used for the first time $\delta^{30}Si_{BSi}$ measured in deep and shallow traps to estimate and monitor seasonal variations of particle sinking speeds in the AZ and PFZ. In these zones, fresh diatoms were exported relatively quickly as phytodetrital aggregates during spring when biological activity increased in the ML. During the summer peak of production in surface water, aggregation and repackaging processes shifted the sinking velocities of particles up to 200 $m\,d^{-1}$ in the AZ. Then, after the demise of the bloom, aggregates were degraded and diatoms were consumed and/or dissolved in the ML leading to a progressive decrease of their settling rates. This study provides by an original approach new data that contribute to corroborate previous hypotheses about the dynamic of the biological production and its export [e.g., *Trull et al*., 2008; *Ebersbach et al*., 2011; *Laurenceau-Cornec et al*., 2015a]. Moreover, it points out a new set of questions about the key role of aggregation/disaggregation processes in the control of particle settling rates and therefore in their influence on the silicon isotopic composition of the BSi that leave the ML and potentially reach the seafloor.

Using seasonal variations of $\delta^{30}Si_{BSi}$ of material collected in deep sediment traps, we had access to other information about processes occurring in the ML and infiltrated the biogeochemical cycle of silicon in the Southern Ocean. This study aims to expand the available $\delta^{30}Si$ data set and highlights once again the relevance to use silicon isotopes in a quantitative way. However, more efforts to quantitatively model processes involved in seasonal variations of $\delta^{30}Si$ and to improve estimates of silicon isotopes dynamics and mass balance in the ocean are necessary. We are currently in the process of refining model based on the approach of *Fripiat et al*. [2012] to better describe the observed $\delta^{30}Si$ seasonal evolution that is not properly described by the conventional Rayleigh or steady state approach.

Acknowledgments

Data for this paper are available in the supporting information Data Set S1. Sediment trap and deployments, augmented by surface biogeochemical and meteorological moorings, are ongoing at the 47°S site under the auspices of the Australian Integrated Marine Observing System (www.imos.org.au). Ocean color analyses and visualizations used in this paper were produced with the Giovanni online data system, developed and maintained by the NASA GES. The research leading to these results has received funding from the European Union Seventh Framework Program under grant agreement 294146 (MuSiCC Marie Curie CIG) and is part of the GEOTRACES program. The SAZ sediment trap program received support from the Australian Antarctic Climate and Ecosystems Cooperative Research Centre, Australian Antarctic Sciences awards 1156 and 2256, the Australian Marine National Facility, the U.S. NSF Office of Polar Programs, and the Belgian Science and Policy Organisation. The authors are especially grateful to Jean-Baptiste Sallée who provided monthly averaged mixed layer depths extracted from the Argo data set and two anonymous reviewers for their constructive comments on the manuscript.

References

Abraham, K., S. Opfergelt, F. Fripiat, A.-J. Cavagna, J. T. M. de Jong, S. F. Foley, L. André, and D. Cardinal (2008), δ30Si and δ29Si determination on USGS BHVO-1 and BHVO-2 reference materials with a new configuration on a Nu plasma multi-collector ICP-MS, *Geostand. Geoanal. Res.*, *32*(2), 193–202.

Armstrong, R. A., C. Lee, J. I. Hedges, S. Honjo, and S. G. Wakeham (2002), A new mechanistic model for organic carbon fluxes in the ocean based on the quantitative association of POC with ballast minerals, *Deep Sea Res., Part II*, *49*, 219–236.

Asper, V. L., and W. O. Smith Jr. (2003), Abundance, distribution and sinking rates of aggregates in the Ross Sea, Antarctica, *Deep Sea Res., Part I*, *50*, 131–150.

Assmy, P., et al. (2013), Thick-shelled, grazer-protected diatoms decouple ocean carbon and silicon cycles in the iron-limited Antarctic Circumpolar Current, *Proc. Natl. Acad. Sci. U.S.A.*, *110*, 20,633–20,638.

Beucher, C. P., M. A. Brzezinski, and J. L. Jones (2008), Sources and biological fractionation of Silicon isotopes in the Eastern Equatorial Pacific, *Geochim. Cosmochim. Acta*, *72*, 3063–3073, doi:10.1016/j.gca.2008.04.021.

Boyd, P. W., and T. W. Trull (2007), Understanding the export of biogenic particles in oceanic waters: Is there consensus?, *Prog. Oceanogr.*, *72*, 276–312.

Boyd, P. W., J. LaRoche, M. Gall, R. Frew, and R. M. L. McKay (1999), Role of iron, light, and silicate in controlling algal biomass in subantarctic waters SE of New Zealand, *J. Geophys. Res.*, *104*(C6), 13,395–13,408, doi:10.1029/1999JC900009.

Boyd, P. W., et al. (2004), The decline and fate of an iron-induced subarctic phytoplankton bloom, *Nature*, *428*, 549–553.

Brzezinski, M. A., D. M. Nelson, V. M. Franck, and D. E. Sigmon (2001), Silicon dynamics within an intense open-ocean diatom bloom in the Pacific sector of the Southern Ocean, *Deep Sea Res., Part II*, *48*, 3997–4018.

Brzezinski M. A., C. J. Pride, and V. M. Frank (2002), A switch from Si(OH)4 to NO3- depletion in the glacial Southern Ocean, *Geophys. Res. Lett.*, *29*(12), 1564, doi:10.1029/2001GL014349.

Buesseler, K. O., et al. (2007), An assessment of the use of sediment traps for estimating upper ocean particle fluxes, *J. Mar. Res.*, *65*, 345–416.

Cardinal, D., F. Dehairs, T. Cattaldo, and L. André (2001), Geochemistry of suspended particles in the Subantarctic and Polar Frontal Zones south of Australia: Constraints on export and advection processes, *J. Geophys. Res.*, *106*(C12), 31,637–31,656, doi:10.1029/2000JC000251.

Cardinal, D., L. Y. Alleman, J. De Jong, K. Ziegler, and L. André (2003), Isotopic composition of silicon measured by multicollector plasma source mass spectrometry in dry plasma mode, *J. Anal. At. Spectrom.*, *18*, 213–218.

Cardinal, D., L. Y. Alleman, F. Dehairs, N. Savoye, T. W. Trull, and L. André (2005), Relevance of silicon isotopes to Si-nutrient utilization and Si-source assessment in Antarctic waters, *Global Biogeochem. Cycles*, *19*, GB2007, doi:10.1029/2004GB002364.

Cardinal, D., N. Savoye, T. W. Trull, F. Dehairs, E. E. Kopczynska, F. Fripiat, J.-L. Tison, and L. André (2007), Silicon isotopes in spring Southern Ocean diatoms: Large zonal changes homogeneity among size fractions, *Mar. Chem.*, *106*, 46–62.

De La Rocha, C. L. (2006), Opal-based isotopic proxies of paleoenvironmental conditions, *Global Biogeochem. Cycles*, *20*, GB4S09, doi:10.1029/2005GB002664.

De La Rocha, C. L., M. A. Brzezinski, and M. J. DeNiro (1997), Fractionation of silicon isotopes by marine diatoms during biogenic silica formation, *Geochim. Cosmochim. Acta*, *61*(23), 5051–5056.

De La Rocha, C. L., M. A. Brzezinski, M. J. DeNiro, and A. Shemesh (1998), Silicon-isotope composition of diatoms as an indicator of past oceanic change, *Nature*, *395*, 680–683.

De Salas, M. F., R. Eriksen, A. T. Davidson, and S. W. Wright (2011), Protistan communities in the Australian sector of the Sub-Antarctic Zone during SAZ-Sense, *Deep Sea Res., Part II*, *58*, 2135–2149, doi:10.1016/j.dsr2.2011.05.032.

De Souza, G. F., R. D. Slater, J. P. Dunne, and J. L. Sarmiento (2014), Deconvolving the controls on the deep ocean's silicon stable isotope distribution, *Earth Planet. Sci. Lett.*, *398*, 66–76.

Ding, T., S. Jiang, D. Wan, Y. Li, J. Li, H. Song, Z. Liu, and X. Yao (1996), *Silicon Isotope Geochemistry*, Geological Publishing House, Beijing, China.

Dong, S., J. Sprintall, S. T. Gille, and L. Talley (2008), Southern Ocean mixed-layer depth from Argo float profiles, *J. Geophys. Res.*, *113*, C06013, doi:10.1029/2006JC004051.

Ebersbach, F., T. W. Trull, D. M. Davies, and S. G. Bray (2011), Controls on mesopelagic particle fluxes in the Sub-Antarctic and Polar Frontal Zones in the Southern Ocean south of Australia in summer—Perspectives from free-drifting sediment traps, *Deep Sea Res., Part II*, *58*, 2260–2276, doi:10.1016/j.dsr2.2011.05.025.

Egan, K. E., R. E. M. Rickaby, M. J. Leng, K. R. Hendry, M. Hermoso, H. J. Sloane, H. Bostock, and A. N. Halliday (2012), Diatom silicon isotopes as a proxy for silicic acid utilisation: A Southern Ocean core top calibration, *Geochim. Cosmochim. Acta*, *96*, 174–192, doi:10.1016/j.gca.2012.08.002.

Elhert, C., P. Grasse, E. Mollier-Vogel, T. Böschen, J. Franz, G. F. de Souza, B. C. Reynolds, L. Stramma, and M. Frank (2012), Factors controlling the silicon isotope distribution in waters and surface sediments of the Peruvian coastal upwelling, *Geochim. Cosmochim. Acta*, *99*, 128–145.

Etourneau, J., C. Ehlert, M. Frank, P. Martinez, and R. Schneider (2012), Contribution of changes in opal productivity and nutrient distribution in the coastal upwelling systems to Late Pliocene/Early Pleistocene climate cooling, *Clim. Past*, *8*, 1435–1445, doi:10.5194/cp-8-1435-2012.

Fripiat, F., A.-J. Cavagna, F. Dehairs, S. Speich, L. André, and D. Cardinal (2011a), Silicon pool dynamics and biogenic silica export in the Southern Ocean inferred from Si-isotopes, *Ocean Sci.*, *7*, 533–547, doi:10.5194/os-7-533-2011.

Fripiat, F., K. Leblanc, M. Elskens, A.-J. Cavagna, L. Armand, L. André, F. Dehairs, and D. Cardinal (2011b), Efficient silicon recycling in summer in both the Polar Frontal and Subantarctic Zones of the Southern Ocean, *Mar. Ecol. Prog. Ser.*, *435*, 47–61, doi:10.3354/meps09237.

Fripiat, F., A.-J. Cavagna, N. Savoye, F. Dehairs, L. André, and D. Cardinal (2011c), Isotopic constraints on the Si-biogeochemical cycle of the Antarctic Zone in the Kerguelen area (KEOPS), *Mar. Chem.*, *123*, 11–22.
Fripiat, F., A.-J. Cavagna, F. Dehairs, A. de Brauwere, L. André, and D. Cardinal (2012), Processes controlling the Si-isotopic composition in the Southern Ocean and application for paleoceanography, *Biogeosciences*, *9*, 2443–2457, doi:10.5194/bg-9-2443-2012.
Fry, B. (2006), *Stable Isotope Ecology*, Springer Science Business Media LLC, New York.
Georg, R. B., B. C. Reynolds, M. Frank, and A. N. Halliday (2006), New sample preparation techniques for the determination of Si isotopic compositions using MC-ICPMS, *Chem. Geol.*, *235*, 95–104.
Goutx, M., S. G. Wakeham, C. Lee, M. Duflos, C. Guigue, Z. Liu, B. Moriceau, R. Sempéré, M. Tedetti, and J. Xue (2007), Composition and degradation of marine particles with different settling velocities in the northwestern Mediterranean Sea, *Limnol. Oceanogr.*, *52*(4), 1645–1664.
Grasse, P., C. Ehlert, and M. Frank (2013), The influence of water mass mixing on the dissolved Si isotope composition in the Eastern Equatorial Pacific, *Earth Planet. Sci. Lett.*, *380*, 60–71.
Grasshoff, K., K. Kremling, and M. Ehrhardt (1999), *Methods of Seawater Analysis*, 3rd completely Revised and Extended edition, Wiley-VCH, Weinheim, Germany.
Grigorov, I., A. Rigual-Hernandez, S. Honjo, A. E. S. Kemp, and L. Armand (2014), Settling fluxes of diatoms to the interior of the Antarctic circumpolar current along 170°W, *Deep Sea Res., Part I*, *93*, 1–13.
Hendry, K. R., L. F. Robinson, J. F. McManus, and J. D. Hays (2014), Silicon isotopes indicate enhanced carbon export efficiency in the North Atlantic during deglaciation, *Nat. Commun.*, *5*, doi:10.1038/ncomms4107.
Holzer, M., F. W. Primeau, T. DeVries, and R. Matear (2014), The Southern Ocean silicon trap: Data-constrained estimates of regenerated silicic acid, trapping efficiencies, and global transport paths, *J. Geophys. Res. Oceans*, *119*, 313–331, doi:10.1002/2013JC009356.
Honjo, S., R. François, S. Manganini, J. Dymond, and R. Collier (2000), Particle fluxes to the interior of the Southern Ocean in the Western Pacific sector along 170°W, *Deep Sea Res., Part II*, *47*, 3521–3548.
Hughes, H. J., C. Delvigne, M. Korntheuer, J. De Jong, L. André, and D. Cardinal (2011), Controlling the mass bias introduced by anionic and organic matrices in silicon isotopic measurements, *J. Anal. At. Spectrom.*, *26*, 1892–1896.
Iversen, M. H., and H. Ploug (2010), Ballast minerals and the sinking carbon flux in the ocean: Carbon-specific respiration rates and sinking velocity of marine snow aggregates, *Biogeosciences*, *7*, 2613–2624, doi:10.5194/bg-7-2613-2010.
Iversen, M. H., and H. Ploug (2013), Temperature effects on carbon-specific respiration rate and sinking velocity of diatom aggregates—Potential implications for deep ocean export processes, *Biogeosciences*, *10*, 4073–4085, doi:10.5194/bg-10-4073-2013.
Kopczynska, E. E., F. Dehairs, M. Elskens, and S. Wright (2001), Phytoplankton and microzooplankton variability between the Subtropical and Polar Fronts south of Australia: Thriving under regenerative and new production in late summer, *J. Geophys. Res.*, *106*(C12), 31,597–31,609, doi:10.1029/2000JC000278.
Laurenceau-Cornec, E. C., T. Trull, D. M. Davies, S. G. Bray, J. Doran, F. Planchon, F. Carlotti, M. Jouandet, A.-J. Cavagna, and A. Waite (2015a), The relative importance of phytoplankton aggregates and zooplankton fecal pellets to carbon export: Insights from free-drifting sediment trap deployments in naturally iron-fertilised waters near the Kerguelen Plateau, *Biogeosciences*, *12*, 1007–1027.
Laurenceau-Cornec, E. C., T. W. Trull, D. Davies, C. L. De La Rocha, and S. Blain (2015b), Phytoplankton morphology controls on marine snow sinking velocity, *Mar. Ecol. Prog. Ser*, *520*, 35–56.
MacDonnell, A. M. P., and K. O. Buesseler (2010), Variability in the average sinking velocity of marine particles, *Limnol. Oceanogr.*, *55*(5), 2085–2096.
Martin, J. H. (1990), Glacial-interglacial CO_2 change: The iron hypothesis, *Paleoceanography*, *5*(1), 1–13, doi:10.1029/PA005i001p00001.
Mosseri, J., B. Quéguiner, L. Armand, and V. Cornet-Barthaux (2008), Impact of iron on silicon utilization by diatoms in the Southern Ocean: A case study of Si/N cycle decoupling in a naturally iron-enriched area, *Deep Sea Res., Part II*, *55*, 801–819.
Nelson, D. M., M. A. Brzezinski, D. E. Sigmon, and V. M. Franck (2001), A seasonal progression of Si limitation in the Pacific sector of the Southern Ocean, *Deep Sea Res., Part II*, *48*, 3973–3995.
Opfergelt, S., and P. Delmelle (2012), Silicon isotopes and continental weathering processes: Assessing controls on Si transfer to the ocean, *C. R. Geosci.*, *344*, 723–738, doi:10.1016/j.crte.2012.09.006.
Orsi, A. H., T. Whiworth III, and W. D. Nowlin Jr. (1995), On the meridional extent and fronts of the Antarctic Circumpolar Current, *Deep Sea Res., Part I*, *42*(5), 641–673.
Panizzo, V., J. Crespin, X. Crosta, A. Shemesh, G. Massé, R. Yam, N. Mattielli, and D. Cardinal (2014), Sea ice diatom contributions to Holocene nutrient utilization in East Antarctica, *Paleoceanography*, *29*, 328–342, doi:10.1002/2014PA002609.
Parslow, J. S., P. W. Boyd, S. R. Rintoul, and F. B. Griffiths (2001), A persistent subsurface chlorophyll maximum in the Interpolar Frontal Zone south of Australia: Seasonal progression and implications for phytoplankton-light-nutrient interactions, *J. Geophys. Res.*, *106*(C12), 31,543–31,557, doi:10.1029/2000JC000322.
Passow, U., R. F. Shipe, A. Murray, D. K. Pak, M. A. Brzezinski, and A. L. Alldredge (2001), The origin of transparent exopolymer particles (TEP) and their role in the sedimentation of particulate matter, *Cont. Shelf Res.*, *21*, 327–346.
Quéguiner, B. (2013), Iron fertilization and the structure of planktonic communities in high nutrient regions of the Southern Ocean, *Deep Sea Res., Part II*, *90*, 43–54.
Ragueneau, O., et al. (2000), A review of the Si cycle in the modern ocean: Recent progress and missing gaps in the application of biogenic opal as a paleoproductivity proxy, *Global Planet. Change*, *26*, 317–365.
Ragueneau, O., N. Savoye, Y. Del Amo, J. Cotten, B. Tardiveau, and A. Leynaert (2005), A new method for the measurement of biogenic silica in suspended matter of coastal waters: Using Si:Al ratios to correct for the mineral interference, *Cont. Shelf Res.*, *25*, 697–710.
Reynolds, B. C., et al. (2007), An inter-laboratory comparison of Si isotope reference materials, *J. Anal. At. Spectrom.*, *22*, 561–568, doi:10.1039/b616755a.
Rigual-Hernández, A. S., T. W. Trull, S. G. Bray, I. Closset, and L. K. Armand (2015a), Seasonal dynamics in diatom export fluxes to the deep sea in the Australian sector of the Antarctic Zone, *J. Mar. Syst.*, *142*, 62–74.
Rigual-Hernández, A. S., T. W. Trull, S. G. Bray, A. Cortina, and L. K. Armand (2015b), Latitudinal and temporal distributions of diatom populations in the pelagic waters of the Subantarctic and Polar Frontal Zones of the Southern Ocean and their role in the biological pump, *Biogeosci. Discuss.*, *12*, 8615–8690.
Rintoul, S. R., and T. W. Trull (2001), Seasonal evolution of the mixed layer in the Subantarctic Zone south of Australia, *J. Geophys. Res.*, *106*(C12), 31,447–31,462, doi:10.1029/2000JC000329.
Sallée, J. B., N. Wienders, R. Morrow, and K. Speer (2006), Formation of subantarctic mode water in the southeastern Indian Ocean, *Ocean Dyn.*, *56*, 525–542.
Sarmiento, J. L., N. Gurber, M. A. Brzezinski, and J. P. Dunne (2004), High-latitude controls of thermocline nutrients and low latitude biological productivity, *Nature*, *427*, 56–60.

Schulz, E. W., S. A. Josey, and R. Verein (2012), First air-sea flux mooring measurements in the Southern Ocean, *Geophys. Res. Lett.*, *39*, L16606, doi:10.1029/2012GL052290.

Siegel, D. A., T. C. Granata, A. F. Micheals, and T. D. Dickey (1990), Mesoscale eddy diffusion, particle sinking, and the interpretation of sediment trap data, *J. Geophys. Res.*, *95*(C4), 5305–5311, doi:10.1029/JC095iC04p05305.

Sigman, D. M., M. A. Altabet, D. C. McCorkle, R. François, and G. Fischer (1999), The δ^{15}N of nitrate in the Southern Ocean: Consumption of nitrate in surface waters, *Global Biogeochem. Cycles*, *13*(4), 1149–1166, doi:10.1029/1999GB900038.

Sigmon, D. E., D. M. Nelson, and M. A. Brzezinski (2002), The Si cycle in the Pacific sector of the Southern Ocean: Seasonal diatom production in the surface layer and export to the deep sea, *Deep Sea Res., Part II*, *49*, 1747–1763.

Stemmann, L., G. A. Jackson, and G. Gorsky (2004), A vertical model of particle size distributions and fluxes in the midwater column that includes biological and physical processes—Part II: Application to a three year survey in the NW Mediterranean Sea, *Deep Sea Res., Part I*, *51*, 885–908.

Sutton, J. N., D. E. Varela, M. A. Brzezinski, and C. P. Beucher (2013), Species-dependent silicon isotope fractionation by marine diatoms, *Geochim. Cosmochim. Acta*, *104*, 300–309.

Thornton, D. (2002), Diatom aggregation in the sea: Mechanisms and ecological implications, *Eur. J. Phycol.*, *37*(2), 149–161, doi:10.1017/S0967086202003657.

Tréguer, P. J., and C. L. De La Rocha (2013), The world ocean silica cycle, *Annu. Rev. Mar. Sci.*, *5*, 477–501.

Trull, T., S. R. Rintoul, M. Hadfield, and E. R. Abraham (2001a), Circulation and seasonal evolution of polar waters south of Australia: Implications for iron fertilization of the Southern Ocean, *Deep Sea Res., Part II*, *48*, 2439–2466.

Trull, T., S. G. Bray, S. J. Manganini, S. Honjo, and R. François (2001b), Moored sediment trap measurements of carbon export in the Subantarctic and Polar Frontal Zones of the Southern Ocean, south of Australia, *J. Geophys. Res.*, *106*(C12), 31,489–31,509, doi:10.1029/2000JC000308.

Trull, T., S. G. Bray, K. O. Buesseler, C. H. Lamborg, S. Manganini, C. Moy, and J. Valdes (2008), In situ measurement of mesopelagic particle sinking rates and the control of carbon transfer to the ocean interior during the Vertical Flux in the Global Ocean (VETIGO) voyages in the North Pacific, *Deep Sea Res., Part II*, *55*, 1684–1695.

Turner, J. T. (2002), Zooplankton fecal pellets, marine snow and sinking phytoplankton blooms, *Aquat. Microb. Ecol.*, *27*, 57–102.

Van den Boorn, S. H. J. M., P. Z. Vroon, and M. J. Van Bergen (2009), Sulfur-induced offsets in MC-ICP-MS silicon-isotope measurements, *J. Anal. At. Spectrom.*, *24*, 1111–1114.

Varela, D. E., C. J. Pride, and M. A. Brzezinski (2004), Biological fractionation of silicon isotopes in Southern Ocean surface waters, *Global Biogeochem. Cycles*, *18*, GB1047, doi:10.1029/2003GB002140.

Weeding, B., and T. W. Trull (2014), Hourly oxygen and total gas tension measurements at the Southern Ocean Time Series site reveal winter ventilation and spring net community production, *J. Geophys. Res. Oceans*, *119*, 348–358, doi:10.1002/2013JC009302.

Yu, E.-F., R. François, M. P. Bacon, S. Honjo, A. P. Fleer, S. J. Manganini, M. M. Rutgers van der Loeff, and V. Ittekot (2001), Trapping efficiency of bottom-tethered sediment traps estimated from the intercepted fluxes of ^{230}Th and ^{231}Pa, *Deep Sea Res., Part I*, *48*, 865–889.